Journal of Power Sources 196 (2011) 3743–3749

Contents lists available at ScienceDirect

Journal of Power Sources

journal homepage: www.elsevier.com/locate/jpowsour

Effects of operating conditions on durability of polymer electrolyte membrane fuel cell Pt cathode catalyst layer

Shinsuke Ohyagi[a,*], Toshihiko Matsuda[a], Yohei Iseki[b], Tatsuyoshi Sasaki[a], Chihiro Kaito[c]

[a] New Energy Device Research Laboratory, KRI, Inc., 5-11-151 Torishima, Konohana-ku, Osaka-City, Osaka 554-0051, Japan
[b] Enviromental Chemical Process Laboratory, KRI, Inc., 5-11-151 Torishima, Konohana-ku, Osaka-City, Osaka 554-0051, Japan
[c] Ritsumeikan University, 1-1-1 Nojihigashi, Kusatsu-shi, Shiga, Japan

ARTICLE INFO

Article history:
Received 31 October 2010
Accepted 16 December 2010
Available online 24 December 2010

Keywords:
Polymer electrolyte fuel cells
Cathode catalyst layer
Pt agglomeration
Voltage cycling
Electrochemical surface area

ABSTRACT

In this study, we investigated the effects of humidity and oxygen reduction on the degradation of the catalyst of a polymer electrolyte membrane fuel cell (PEMFC) in a voltage cycling test. To elucidate the effect of humidity on the voltage cycling corrosion of a carbon-supported Pt catalyst with 3 nm Pt particles, voltage cycling tests based on 10,000 cycles were conducted using 100% relative humidity (RH) hydrogen as anode gas and nitrogen of varying humidities as cathode gas. The degradation rate of an electrochemical surface area (ECSA) was almost 50% under 189% RH nitrogen atmosphere and the Pt average particle diameter after 10,000 cycles under these conditions was about 2.3 times that of a particle of fresh catalyst because of the agglomeration of Pt particles.

The oxygen reduction reaction (ORR) that facilitated Pt catalyst agglomeration when oxygen was employed as the cathode gas also demonstrated that Pt agglomeration was prominent in higher concentrations of oxygen. The ECSA degradation figure in 100% RH oxygen was similar to that in 189% RH nitrogen. It was concluded that liquid water, which was dropped under a supersaturated condition or generated by ORR, accelerated Pt agglomeration. In this paper, we suggest that the Pt agglomeration degradation occurs in a flooding area in a cell plane.

1. Introduction

Polymer electrolyte membrane fuel cells (PEMFCs) are expected to have applications as a clean power source for vehicles. At present, PEMFCs developed thus far work on a practical scale. However, further improvements are necessary to enhance their durability in order to make operation on a commercial scale viable. For vehicles, operation modes, such as running, stopping, idling, and parking modes, all impact on catalyst degradation to varying degrees. In order to improve PEMFC durability it is important to understand how start/stop operations and load changing influence the degradation mechanism to. One of the major deterioration factors considered is changing the electrochemical potential of the catalyst layer with load changing. Platinum corrosion rates in fuel cells have been observed to increase when the catalyst is exposed to high voltage [1–4], particularly when the cell voltage is cycled [5,6].

It is known that voltage cycling of carbon supported platinum (Pt/C) in aqueous acids at room temperature leads to accelerated platinum dissolution rates compared to extended holds at constant potentials [5,7]. Johnson et al. reported that Pt(II) is produced when an oxidized platinum electrode is reduced [8], and it is assumed that a greater number of oxide formation–reduction cycles per unit time leads to a greater instability of Pt. [3,8]. Ross [9] conceptualizes platinum coarsening and area loss at two different length scales, viz. (i) a nanometer-scale Ostwald-ripening process, where smaller platinum particles dissolve in the ionomer phase and redeposit on larger platinum particles that are separated by a few nanometers; and (ii) a micrometer-scale diffusion process, where dissolved platinum ions diffuse toward the matrix and undergo reduction on the anode side at low potentials. Paik et al. investigated the effect of time periods and lower voltage level as cycling parameters on catalyst stability. Their cycling parameters have been found to impact the rate of decay in platinum electrochemical area (ECSA) at the same cumulative time of exposure to the high voltage level (1.3 VRHE). A higher frequency cycling of 0.5–1.3 VRHE was found to accelerate the decay rate of Pt ECSA. ECSA loss is due to the growth in platinum particle size. When the lower voltage was set above the Pt oxide reduction potential, the rate of ECSA loss was found to decrease. It suggests that Pt dissolution rates decelerate due to a partially remaining passive film [10].

Platinum corrosion rates in fuel cells have been observed to increase when the catalyst is exposed to high humidity in the same voltage cycling tests [11]. H_2–N_2 PEM systems were carried out to investigate the effects of potential and humidity for electrocatalyst

* Corresponding author. Tel.: +81 6 6464 9237; fax: +81 6 6464 9238.
E-mail address: ohyagi@kri-inc.jp (S. Ohyagi).

0378-7753/$ – see front matter © 2010 Elsevier B.V. All rights reserved.
doi:10.1016/j.jpowsour.2010.12.068

Table 1
Operation conditions of voltage cycling test.

		Effects of	
		Humidity	ORR
Catalyst		Carbon-supported Pt electrochemical catalyst with Pt weight ratio of about 50 wt%	
PEM		Nafion N112	
Cell temperature		75 °C	
Gas species/relative humidity	Anode	H_2/100% RH	
	Cathode	N_2/20%, 100%,189% RH	N_2, 4%-O_2, 100%-O_2/100% RH
Potential sweep range		0.4–1 V vs. RHE	
Potential sweep rate		50, 200 mV s^{-1}	50 mV s^{-1}
Number of cycles		10,000, 50,000 cycles	10,000 cycles

corrosion in previous reports [1,10–12]. Although these methods reasonably accounted for the degradation mechanism of the electrocatalyst layer in voltage cycling test, it may not be possible to extrapolate this mechanism to an actual fuel cell system. In the cell plane, especially the cathode side of the actual fuel cell stack, the proportion of water is increases from the gas inlet to the exit as a result of an oxygen reduction reaction. The condensed water will be generated as the result of high current density operation for automotive fuel cell. Previous reports verified the effect of humidity below 100% RH, but did not focus on the influence of condensed liquid water on electrocatalyst corrosion. Although N_2 cathode gas in the voltage cycling test would clarify the effect of voltage or humidity without ORR, the oxygen reduction reaction still occurs at the cathode in normal fuel cell operations. Because water is generated by the ORR, it is not obvious whether the electrocatalyst corrosion is accelerated by ORR or by high humidity conditions resulting in ORR. It is important to clarify the contribution of ORR to electrocatalyst corrosion.

Herein, we examined the effect of cell operating humidity conditions, especially condensed liquid water on the durability of a PEMFC cathode catalyst layer in the load changing operation mode of vehicles using a single cell. At the same time, we attempted to consider the effect of oxygen reduction reaction (ORR) and the water generated by ORR on the durability of PEMFC.

2. Experimental

2.1. Preparation

The membrane electrode assembly (MEA) was prepared by a decal method by hot pressing Nafion N112 between two catalyst layer decal sheets at 140 °C. These decal sheets were prepared by printing catalyst ink, mixing an ionomer (Du Pont 20 wt% Nafion solution) and a commercial carbon-supported Pt electrocatalyst with a Pt weight ratio of about 50 wt% on a PTFE substrate. Porous carbon papers (SGL Carbon GDL24BC) were used as gas diffusion media and current collectors. The Pt loading in the catalyst layer was 0.4 mgPt cm^{-2}. Two electrode sizes, namely, 6.25 cm^2 and 25 cm^2, were used.

2.2. Voltage cycling test

The prepared MEAs were set in a custom-made PEMFC single cell kit, and the single cell was installed into the PEMFC test stand. We controlled gas flow rate, cell temperature, reactant gas humidity, and cathode electrode sweep potential using a potentiostat/galvanostat and a function generator to simulate the load changing of PEMFC vehicles.

Table 1 shows the operation conditions of our test. The upper scanning voltage was set to 1 V to simulate open circuit voltage (OCV), and the lower scanning voltage was set to 0.4 V to simulate the overload condition. The anode was used as both the reference and counter electrodes by introducing the fully humidified hydrogen into the anode side gas channel, and the potential of the cathode was swept from 0.4 V to 1 V versus the anode as RHE with a 50 mV s^{-1} sweep rate.

We selected cathode gas on the basis of the objectives of the test. We selected nitrogen (N_2) as the first cathode gas to examine the effect of humidity on catalyst layer degradation in the absence of the ORR effect. We conducted tests with three relative humidities, namely, 20% RH, 100% RH, and 189% RH. 189% RH denotes that the cathode gas was humidified at a 91 °C dew point by a bubbling humidifier against a 75 °C cell temperature. In other words, the cathode side was maintained under a supersaturated condition. First, we conducted a 10,000-cycle test and performed cyclic voltammetry (CV) and polarization property every 2000 cycles up to 10,000 cycles. We adopted small size MEA (6.25 cm^2) because the current density of polarization property was limited by our electrochemical test equipment.

We conducted a 50,000-cycle test for vehicle operation mode. In this test, we adopted a more rapid sweep rate (200 mV s^{-1}) to examine the effects of both the cycle number and the sweep rate. We also conducted the voltage cycling test under the same conditions with larger size MEA (25 cm^2) for convenience of estimation of ECSA.

We selected oxygen of various concentrations as the second cathode gas to investigate the effect of ORR on catalyst degradation. We chose 4% oxygen/nitrogen balance gas (4%-O_2) and 100% oxygen gas (O_2). The humidity was maintained at 100% RH. We compared the degrees of degradation at various oxygen gas concentrations.

2.3. Electrochemical diagnostic

ECSA were calculated from electric charge for hydrogen absorption/desorption. We evaluated hydrogen adsorption/desorption by CV using the potentiostat/galvanostat and the function generator. The cell was maintained at 30 °C and the anode side was exposed to humidified hydrogen acting as a reversible hydrogen electrode (RHE). The cathode side was exposed to humidified nitrogen. The voltage was swept from 0.05 to 0.9 V at a rate of 50 mV s^{-1}. Using a proportionality constant of 210 μC cm^{-2} for platinum metal, the charge can be converted to a surface area [13,14]. After the resistance correction, ECSA (S (cm^2 g^{-1})) was calculated using the following equation:

$$ECSA = \frac{Q}{210\,(\mu C\,cm^{-2}) \times dV/dt \times L} \quad (1)$$

where Q (C) is the hydrogen desorption charge, $dV\,dt^{-1}$ (mV s^{-1}) is the scan rate, and L is the cathode Pt loading (mg cm^{-2}). Theoretically, hydrogen desorption charge is the same as hydrogen adsorption charge. Because it is difficult to separate hydrogen adsorption charge from hydrogen generation charge using CV in this method, we adopt the hydrogen desorption charge as Q.

In 10,000-cycle tests, the polarization curves were obtained to evaluate the effect of voltage cycling on electrocatalyst activity. In these polarization tests, the anode side was exposed to 100% RH humidified hydrogen and the cathode side was exposed to 100% RH humidified oxygen to evaluate the electrocatalyst activity without diffusion polarization. The flow rates of H_2 and O_2 were 100 and 400 N mL min^{-1}, respectively, and the cell was maintained at 75 °C. We regulated the current per 1 g of Pt at 0.9 V of the polarization curve as a mass activity, and plotted these mass activities as a function of cycle number.

2.4. Transmission electron microscopy (TEM) analysis

A sample of powder was scraped away and collected with a razor blade from the cathode surface of the fresh and cycled MEAs. MEA samples were examined and compared using TEM. Powders were first immersed in solvent and subsequently ultrasonicated under high frequency to disperse the powder particles. The suspensions were then deposited on a carbon/copper grid for TEM observation. Measurements of 100 randomly selected spherically shaped particles were made for each distribution. We investigated the effect of the humidity and ORR on the size distribution in the voltage cycling tests.

2.5. Platinum solubility measurements in drain

The amounts of soluble Pt in drains were analysed during 10,000 cycle voltage cycling tests. Drains were collected after voltage cycling tests, and soluble Pt concentrations in these drains were analysed by the ICP method. The amount of soluble Pt was calculated from the concentration of Pt and total weight of drain water in the test term.

3. Results and discussion

The voltage cycling test using the humidified N_2 as cathode gas to evaluate the effect of humidity is described first. We then present a discussion regarding the voltage cycling test using various oxygen gas concentrations to evaluate the effect of ORR on the degradation of the catalyst.

3.1. Voltage cycling test using humidified N_2 as cathode gas

The voltage cycling tests using the humidified N_2 as cathode gas were carried out to evaluate the effect of humidity without the effect of water generation by ORR.

We found that higher humidity accelerated the degradation of ECSA, particularly under supersaturated conditions; for example, under a liquid water condition, ECSA decreased more rapidly. Fig. 1 shows the change in ECSA with voltage cycling tests under various humidity conditions. ECSAs were calculated from electrical charges of H desorption of CV obtained every 2000 cycles of the voltage cycling tests using 20% RH, 100% RH and 189% RH N_2 cathode gases. It was clearly found that ECSAs were reduced by cycling under all the humidity conditions employed. These results indicate that one (or a combination) of the following degradation mechanisms occurs to reduce ECSA: Pt agglomeration, Pt elimination, or Pt movement. The Pt surface is oxidized and reduced in this range of voltage change such that a Pt surface change affects the ECSA degradation. The degradation rates of ECSA after the 10,000-cycle test are about 79% with 20% RH N_2, 75% with 100% RH N_2 and 50% with 189% RH N_2. These results indicate that the rate of degradation is faster at higher humidity, and the decrease in ECSA under a supersaturated condition, such as 189% RH, is accelerated.

Fig. 2 shows transmission electron microscopy (TEM) images of the catalyst layer and diameter distributions of Pt before and after voltage cycling tests under an inert atmosphere. These TEM images indicate that the mechanism of ECSA degradation is the agglomeration of Pt particles. In the TEM images, we observed that Pt agglomeration occurs under higher humidity conditions. In particular, Pt agglomeration is accelerated under the supersaturated condition. We determined that the average Pt particle diameter of the fresh catalyst is approximately 3.0 nm with a standard deviation (σ) of 0.59 nm. The average Pt particle diameters after 10,000 cycles with 20% RH N_2 and after 10,000 cycles with 189% RH N_2 are approximately 4.5 nm (σ 1.34 nm) and approximately 7.0 nm (σ 2.79 nm), respectively.

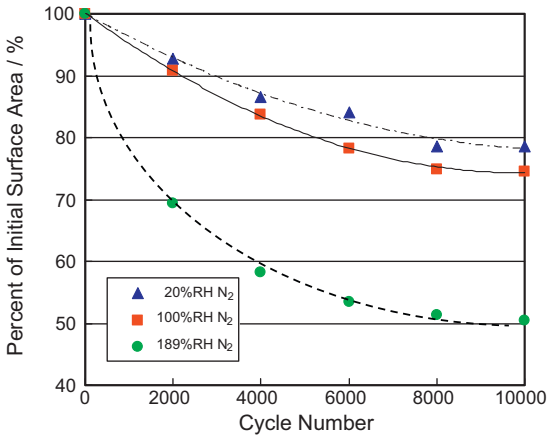

Fig. 1. Impact of relative humidity on Pt/C decay. The percent of ECSA is plotted as a function of cycle numbers. Voltage cycling involved triangle waves at 50 mV s^{-1} between an upper voltage of 1.0 V and a lower voltage of 0.4 V. The voltage cycling was conducted with fully humidified H_2 for anode and 20% RH N_2 (solid triangle), 100% RH N_2 (solid square), and 189% RH N_2 (solid circle) for cathode at 75 °C.

In the voltage cycling test using 189% RH N_2, the cell voltage at a lower current density, such as 10 mA cm^{-2}, decreased so markedly that we assumed it resulted in a lower catalyst activity. Fig. 3 shows the polarization curves for the voltage cycling tests (a) with 20% RH N_2 gas and (b) 189% RH N_2 gas. Both of polarization tests were carried out at 100% RH. We employed oxygen as cathode gas to eliminate diffusion polarization and evaluate only catalyst activity polarization in this IV test. In the case of the voltage cycling test using 20% RH N_2, deviations in cell voltages at 20–100 mA cm^{-2} were within a 10% decrease range. In contrast, the cell voltage decreased markedly in the voltage cycling test using 189% RH N_2. Fig. 4 shows mass activities at 0.9 V in the voltage cycling tests. The mass activity in the 189% RH cycling test was reduced by a greater extent in comparison to that in the 20% RH cycling test. The mass activities showed a similar behavior to the ECSA with cycling. We considered that this mass activity degradation reduced the catalyst activity because of the degradation of ECSA.

Thus, we determined that the degradation of ECSA in a voltage cycling test is caused by Pt agglomeration, and this agglomeration is accelerated under a supersaturated condition. Moreover, we realized that Pt agglomeration reduces both ECSA and cell performance. Considering these phenomena on the cell electrode plane; Pt agglomeration is presumed to occur and accelerate in the flooding area because of poor water management in a cell operation.

We conducted 50,000-cycle tests in 189% RH N_2 to evaluate the effect of cycle number on ECSA degradation. We adopted a sweep rate of 200 mV s^{-1} to examine the effect of sweep speed on ECSA degradation. CVs up to 50,000 cycles are illustrated in Fig. 5. Above 10,000 cycles, ECSA decreases with increasing the number of voltage cycling. Fig. 6 shows the percent of initial ECSA during voltage cycling tests. We plotted ECSAs in 189% RH N_2 with different MEA sizes and sweep rates: (a) 6.25 cm^2, 50 mV s^{-1}: (b) 6.25 cm^2, 200 mV s^{-1}: (c) 25 cm^2, 200 mV s^{-1}: (d) re-test of condition (c).

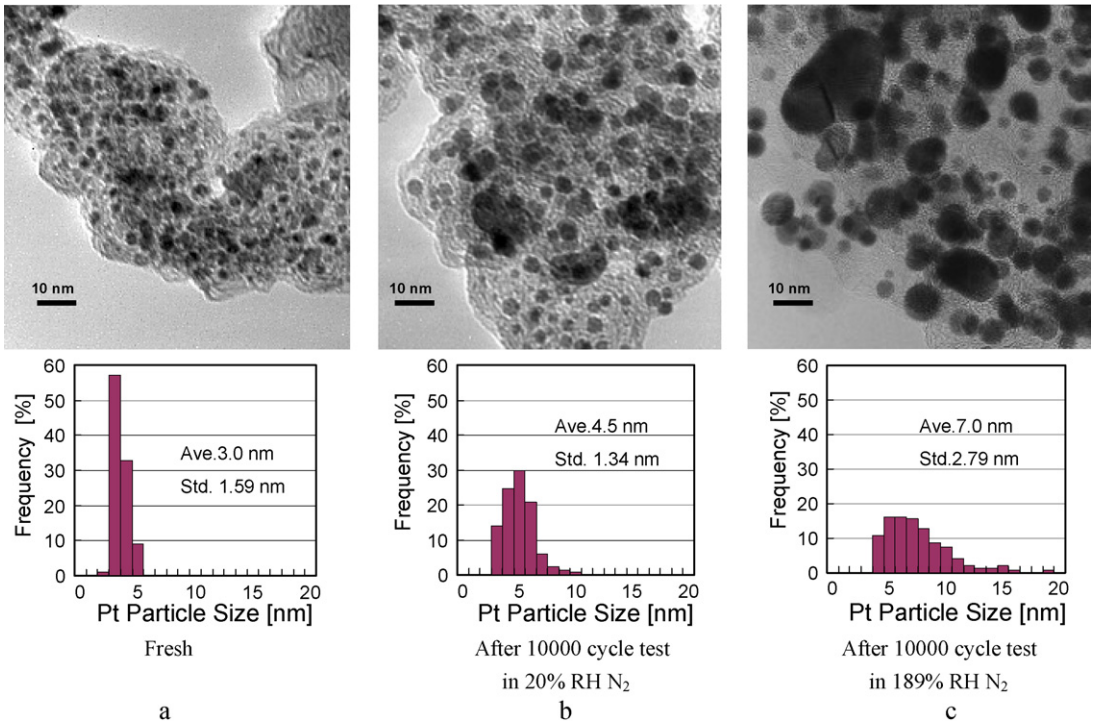

Fig. 2. Typical TEM micrographs from powders scraped away from the cathode surface of (a) fresh MEA sample, (b) the 10,000 cycled MEA sample in 20% RH N_2, and (c) the 10,000 cycled MEA sample in 189% RH N_2. Measurements of 100 randomly selected spherically shaped particles were carried out for each distribution. Considerable coarsening of spherically shaped platinum nanoparticles was found after potential cycling, especially in supersaturated condition (Ave.: average Pt particle diameter, Std.: standard deviation of Pt particle diameter).

Comparing (b) and (c), both ECSAs after 10,000 cycles and 50,000 cycles were about 50% and 37% of initial ECSAs, respectively, in spite of the different MEA sizes. These results suggest that the MEA size does not influence the degradation of Pt/C in the voltage cycling test with inert gas. Comparing (a) and (b), both ECSAs after 10,000 cycles were about 50% of initial ECSAs in spite of different sweep rates. We supposed that cycle number has a stronger impact on Pt agglomeration than sweep rate. We carried out a re-test of 50,000 voltage cycling test with 25 cm^2, 200 $mV\,s^{-1}$ in order to confirm the rate of degradation of the catalyst. ECSA decreased over 10,000 cycles and reached 36% of its initial value after 50,000 voltage cycles. We determined that cycle number has a stronger impact on Pt agglomeration than sweep rate and MEA size in the voltage cycling test. According to previous studies, the electrochemical oxidation of platinum by water, $Pt + H_2O \rightarrow Pt\text{–}OH + H^+ + e^-$, begins to occur at 0.7 V vs. RHE [15–17]. Because Pt agglomeration depends on cycle number and accelerates under a supersaturated condition with exposure to the condensed liquid water, we expect that the reduction/oxidation changes of the Pt surface by water in the potential cycle will induce Pt agglomeration.

3.2. *Voltage cycling test using 4%-O_2 and O_2 as cathode gas*

Subsequently, we attempted to determine the effect of an oxidizer on Pt agglomeration to examine its dependence on ORR. Because ORR depends on the state of three-phase boundaries of the catalyst layer, we conducted voltage cycling tests using 4%-O_2 and O_2 as cathode gas. Humidity was maintained at 100% RH, and tests we conducted under identical sweep rate, sweep voltage, and cell size.

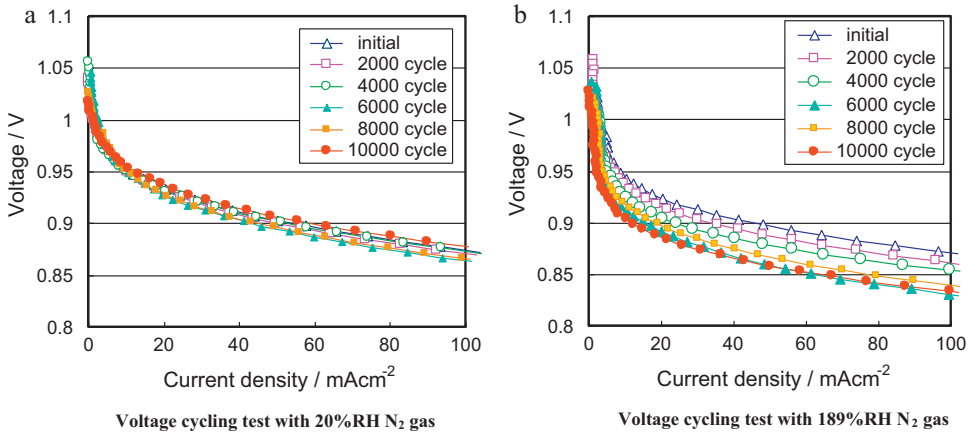

Fig. 3. H_2/O_2 polarization curves of MEA after voltage cycling every 2000 cycles (a) with 20% RH N_2 gas and (b) with 189% RH N_2 gas. The flow rates of H_2 and O_2 were 100 and 400 N mL min^{-1}, respectively, and both gases were humidified at 100% RH. The cell temperature was kept at 75 °C.

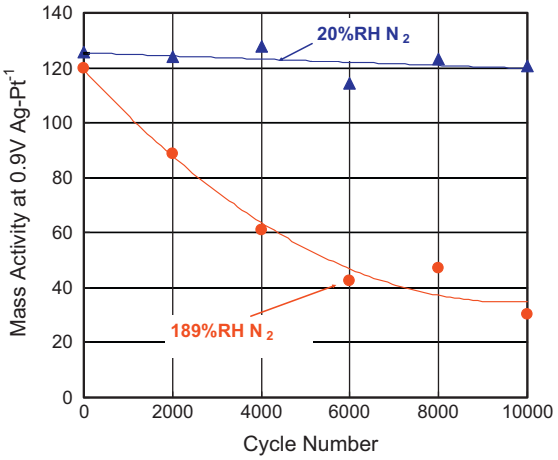

Fig. 4. Impact of relative humidity on mass activities. Mass activities, which were regulated the current per one gram of Pt at 0.9 V, were plotted as a function of cycle numbers. Solid triangle: the mass activities after voltage cycling test with 20% RH N_2 as cathode gas and solid circle: with 189% RH N_2 as cathode gas. The mass activity decay was larger after voltage cycling test with 189% RH as cathode gas.

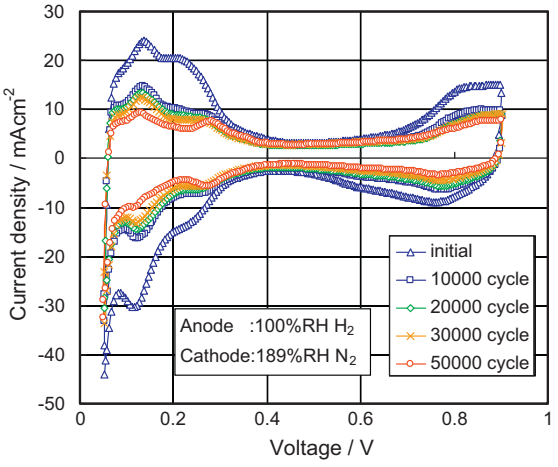

Fig. 5. CV of MEA after voltage cycling every 10,000 cycles up to 50,000 cycles with 189% RH N_2 as cathode gas. CVs were conducted at 30 °C, with fully humidified H_2 and N_2, for anode and cathode gases, respectively. Both flow rates were 100 N mL min^{-1}. The sweep rate was 50 mV s^{-1} and sweep voltage vs. RHE was between 0.05 and 0.9 V.

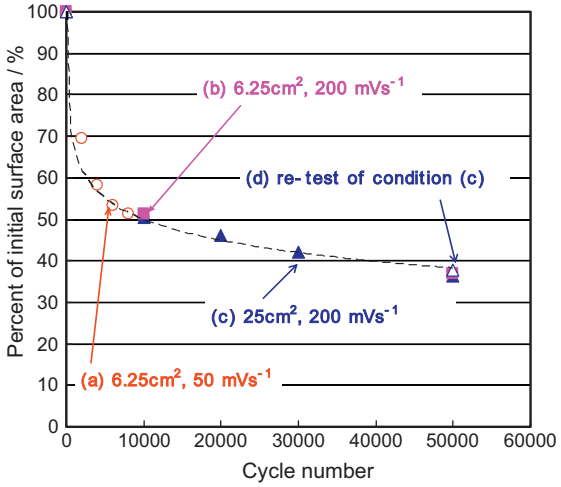

Fig. 6. Percent of initial ECSA during cycling test comparing cell sizes and sweep rates. Solid triangle: 25 cm^2, 200 mV s^{-1} and open circle: 6.25 cm^2, 50 mV s^{-1}. Cathode gases were 189% RH N_2. Although voltage cycling tests were performed in different cell sizes and sweep rates, percent of initial ECSAs were substantially same after 10,000 cycling tests and were plotted on the same decay curve.

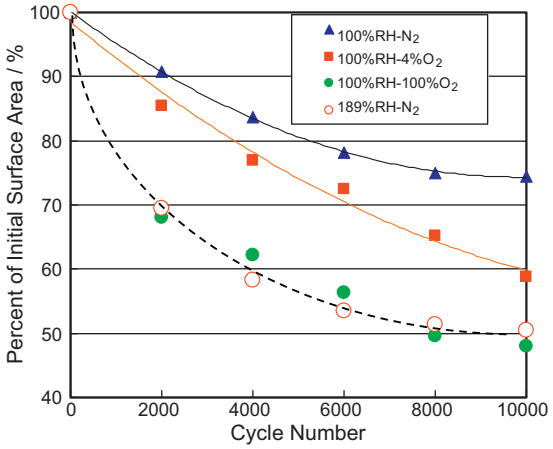

Fig. 7. Impact of O_2 concentration on Pt/C decay. The voltage cycling was conducted with fully humidified H_2 for anode and fully humidified N_2 (solid triangle), 4% O_2 balanced N_2 (solid square), and 100% O_2 (solid circle) for cathode at 75 °C. ECSA of voltage cycling test with 189% RH N_2 is plotted comparing with ECSA with 100% O_2.

Fig. 7 shows the change in ECSA with voltage cycling tests at different oxygen gas concentrations, 100% RH 4%-O_2, 100% RH O_2, 100% RH N_2, and 189% RH N_2 as cathode gas. Degradation to 75% of the initial value was observed after the 10,000-cycle test using N_2 as cathode gas, whereas a degradation to 60% of its initial value was observed after the 10,000-cycle test using 4%-O_2. After the 10,000-cycle test using O_2 as cathode gas, it changed to 50% of its initial value. Thus, ORR may accelerate ECSA degradation in the voltage cycle.

Comparison of the changes in ECSA in voltage cycling tests with 100% RH O_2 gas and 189% RH N_2 as cathode gas show that ECSA degradation behavior in the voltage cycle was similar under both the test conditions. From this result, it is highly possible that Pt agglomeration mechanisms under both the test conditions are the same. We initially had some expectations that the degradation mechanism would be different under ORR conditions and under inert atmosphere and that the rate degradation would be accelerated by ORR. Therefore, our expectation was that Pt agglomeration after the voltage cycling test with 100% RH O_2 would be more noticeable than after the voltage cycling test with supersaturated inert atmosphere because the both test conditions are supersaturated. However, ECSA decays were similar under both the test conditions. This result suggests the possibility that ORR itself might not accelerate the degradation but the supersaturated condition which is caused by ORR in the voltage cycling test with 100% RH O_2 might accelerate Pt agglomeration. Assuming that the MEA temperature is constant, the water which is generated by ORR condensed into liquid phase water in the MEA and the flow channel in the voltage cycling tests with 100% RH O_2 as a cathode gas. The voltage cycling test with 100% RH O_2 as a cathode gas represents the tests under supersaturated conditions.

We believe that the accelerated catalyst degradation can be ascribed both to Pt oxidation by water and to the increased Pt ion transport in large water channel networks by liquid water within polymer electrolyte. A study by Bi et al. measured cyclic voltammetry to quantify the effects on humidity on platinum electrochemical oxidation by water and found notably positive effects of temperature and humidity on platinum electrochemical oxidation [18]. Paik et al. [19] and Xu et al. [15] reported that high temperature and higher humidity resulted in greater importance of electrochemical oxidation by water over gaseous oxygen. These results suggest that the Pt surface is more easily oxidized by water and that Pt(II) is produced in greater amounts when an oxidized Pt electrode is reduced in voltage cycling test under the supersatu-

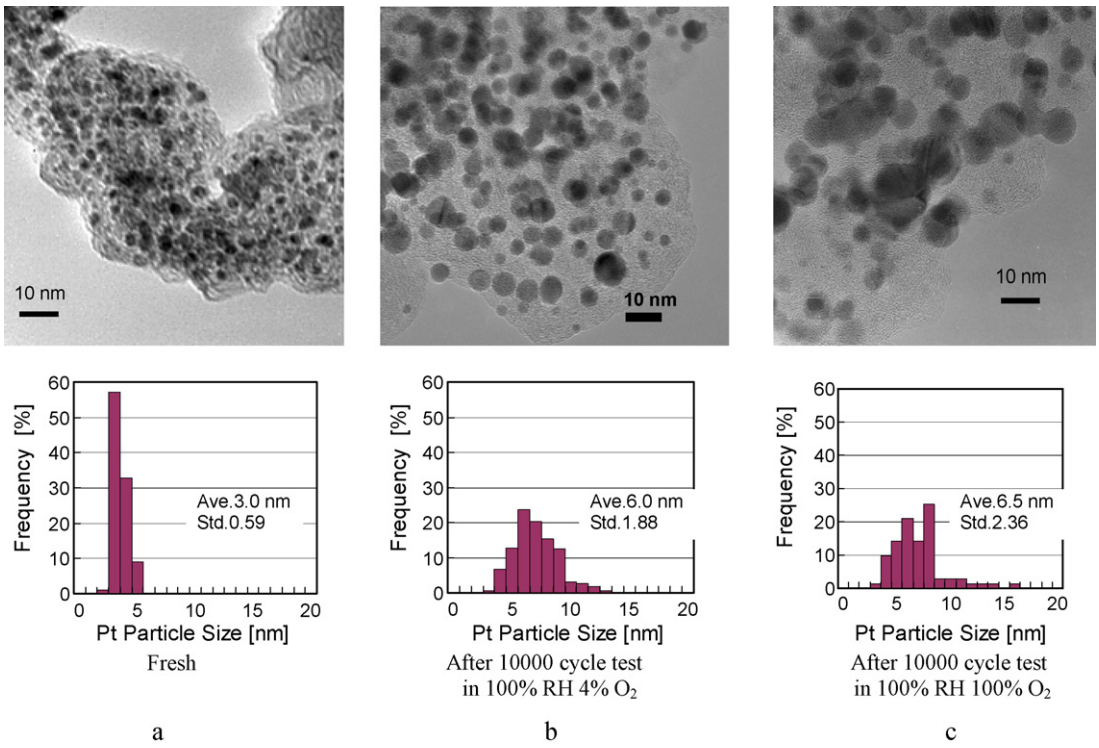

Fig. 8. Typical TEM micrographs from powders scraped away from the cathode surface of (a) fresh MEA sample, (b) the 10,000 cycled MEA sample with 100% RH 4%-O_2, and (c) the 10,000 cycled MEA sample with 100% RH O_2. Size distributions of platinum nanoparticles of each powder scraped from MEA cathode surfaces. Measurements of 100 randomly selected spherically shaped particles were made for each distribution. Considerable coarsening of spherically shaped platinum nanoparticles was found after potential cycling, especially in higher O_2 concentration condition.

rated condition. Bi et al. reported that the effects of oxygen partial pressure on cathode degradation were insignificant, and that the faster cathode degradation rates could be accounted for by the accelerated Pt ion transport in polymer electrolyte at high humidity or high membrane water content due to possibly larger and more abundant water channel networks [18]. Weber and Newman conducted a physical model study demonstrating that the uptake of water increases for the liquid-equilibrated membrane because it possesses enough pressure and energy to infiltrate and expand the channels. Conversely, water vapor does not have enough energy to condense in the channels due to their hydrophobicity, and consequently it has a lower water content [20]. These reports suggests our assumption that ORR itself might not accelerate the degradation but the supersaturated condition caused by ORR in the voltage cycling test with 100% RH O_2 might accelerate Pt agglomeration.

However contrary to the Bi et al.'s result that the oxygen partial pressure did not affect on cathode degradation [18], the degree of Pt agglomeration was larger with high oxygen partial pressure atmosphere in our voltage cycling test. The discrepancy in results may be accounted for by the different test conditions employed. Bi et al.'s voltage cycling test was performed between 0.87 and 1.2 V vs. RHE [18]. Due to the fact that the lower voltage of voltage cycling test was set above the Pt oxide reduction potential, little water was generated by ORR and the humidity was almost constant at 100% RH in spite of various O_2 concentrations for cathode gas. On the other hand, our test was performed between 0.4 and 1.0 V vs. RHE. Because the lower voltage of voltage cycling test was set below the Pt oxide reduction potential, the amount of water, which was generated by ORR, was larger with increasing O_2 concentration for cathode gas. Thus, the differences in membrane water content was caused by the different amount of generated water, and resulted in the different degree of Pt degradation.

TEM images and Pt particle diameter distributions of the catalyst before and after voltage cycling tests are shown in Fig. 8. The average diameter of Pt particle after the 10,000-cycle test in 4%-O_2 and the 10,000-cycle test in O_2 are 6.0 nm (σ 1.88 nm) and 6.5 nm (σ 2.36 nm), respectively. Pt agglomeration progressed with oxygen concentration. This trend is similar to the behavior observed for ECSA degradation. The average particle diameter after the 10,000 voltage cycling test in O_2 (6.5 nm) is similar to that in 189% RH N_2 (7.0 nm) in the degree of Pt agglomeration. This result is in good agreement with the ECSA degradation behavior.

We considered that Pt agglomeration depends on the cycle number of a voltage cycling test, and the Pt surface state is affected by Pt agglomeration. On the basis of these considerations, it is highly probable that the mechanisms of Pt agglomeration are dissolution and redeposition. We attempted to perform a quantitative analysis of Pt in a cathode drain to determine whether Pt dissolution occurs. Fig. 9 shows the results of the quantitative analysis of Pt in the 10,000 voltage cycling test in the cathode drain using 189% RH N_2 and in the both drains using 100% RH O_2. The amounts of Pt shown in Fig. 9 indicate cumulative values. The amount of Pt increased in proportion to cycle number. Table 2 shows dissolution ratios of Pt in the cathode drain using 189% RH N_2, using 100% RH O_2, and in the anode drain using 100% RH O_2. Pt dissolution ratio was defined as:

$$\text{Pt dissolution ratio} = \frac{\text{The amount of Pt in drain [mg]}}{\text{The amount of Pt in catalyst layer of fresh MEA [mg]}} \quad (1)$$

The Pt dissolution ratios in the cathode drain after the 10,000 voltage cycling tests with 189% RH N_2 and 100% RH O_2 were 0.0914% (914 ppm), and 0.0604% (604 ppm), respectively. On the other hand, the Pt dissolution ratio was only slightly detected 0.0104% (104 ppm) in the anode drain with 100% RH O_2. Because Pt dissolution species were detected mainly in the cathode drain, Pt dissolution occurred in voltage cycling test, but the amount

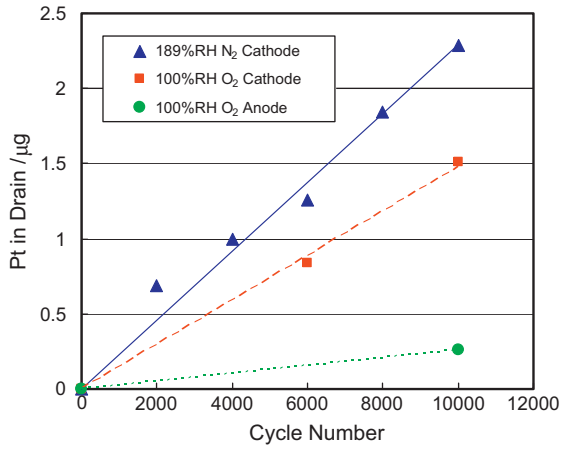

Fig. 9. Analysis of the amount of soluble Pt in drain during 10,000 cycles of voltage cycling test. Cumulative amounts of Pt are plotted as a function of cycling number. Soluble Pt concentration in drain was analysed by ICP method. The amount of soluble Pt was calculated from the concentration of Pt and total weight of drain water in the test term. Solid triangle: cathode drain with 189% RH N_2, solid square: cathode drain with 100% RH O_2, and solid circle: anode drain with 100% RH O_2.

Table 2
Summaries of dissolution rates of Pt after voltage cycling tests.

Test	Σ_w Pt [μg]	Dissolution rate of Pt [ppm]
Cathode in 189% RH N_2 test	2.3	914
Cathode in 100% RH O_2 test	1.5	604
Anode in 100% RH O_2 test	0.3	104

of Pt dissolution after the 10,000-cycle test was in the order of ppm of initial Pt content. In the quantitative analysis of Pt in the drain after the voltage cycling test, only Pt exhausted from MEA was detected. Other Pt dissolution species were possibly deposited in the electrolyte (ionomer or membrane) and in diffusion media. Some reports indicate that the deposited Pt forms a Pt band in the membrane [18,21,22]. From this result, Pt dissolution species generated by the voltage cycling test were probably deposited on Pt particles produced by Pt agglomeration or in the electrolyte, such as the membrane or ionomer.

4. Conclusion

The effects of humidity, especially that because of condensed liquid water, on the durability of PEMFC cathode catalyst layer in the voltage cycling test were investigated. It was shown that ECSA decreased more rapidly under conditions of higher humidity and also decreased markedly in a supersaturated atmosphere, namely, in the presence of liquid water. We concluded that Pt agglomeration, which causes ECSA degradation, in a supersaturated atmosphere caused a significant reduction in cell performance. Pt agglomeration depended on cycle number rather than on the sweep rates of potential, thus, the cycle of the oxidation and reduction of the Pt surface causes Pt agglomeration, and Pt surface can be easily oxidized by water in supersaturated conditions.

We conducted voltage cycling tests using oxygen of various concentrations as the cathode gas to examine the effect of ORR. ECSA degradation was accelerated using oxygen gas and increased in magnitude with increasing oxygen gas concentration. ECSA degradation after the 10,000 voltage cycling test using 100% RH O_2 gas was similar to the level of deterioration observed when using 189% RH N_2. This result was supported by TEM observations of the catalyst layer after voltage cycling tests. Thus, it can be concluded that water generation by ORR accelerated Pt agglomeration in the voltage cycling test using O_2.

These results suggest that Pt agglomeration occurs easily in the flooding area of the cell plane under the load changing operation mode. Further, they suggest that it is imperative to develop an electrode or MEA that cannot be flooded and that can control the rate of Pt agglomeration. These targets can be achieved by setting the operation mode to prevent the electrode from reaching high potential under water condensation, even with a novel electrode or MEA (i.e., purging with dry gas at high potentials or installing a dummy load to a lower potential).

Acknowledgments

This work was supported by the New Energy and Industrial Technology Development Organization (NEDO) in Japan, and was conducted jointly with the Daido Institute of Technology. The authors thank Prof. Hori (Daido Institute of Technology) for technical support.

References

[1] P.J. Ferreira, G.J. la O', Y. Shao-Horn, D. Morgan, R. Makharia, S. Kocha, H.A. Gasteiger, J. Electrochem. Soc. 152 (2005) A2256.
[2] P. Bindra, S.J. Clouser, E. Yeager, J. Electrochem. Soc. 126 (1979) 1631.
[3] X. Wang, R. Kumar, D.J. Myers, Electrochem. Solid-State Lett. 9 (2006) A225.
[4] R.M. Darling, J.P. Meyers, J. Electrochem. Soc. 150 (2003) A1523.
[5] K. Kinoshita, J.T. Lundquist, P. Stonehart, J. Electroanal. Chem. Interfacial Electrochem. 48 (1973) 157.
[6] R.M. Darling, J.P. Meyers, J. Electrochem. Soc. 152 (2005) A242.
[7] B. Merzougui, S. Swathirajan, J. Electrochem. Soc. 153 (12) (2006) A2220.
[8] D.C. Johnson, D.T. Napp, S. Bruckenstein, Electrochim. Acta 15 (1970) 1493.
[9] P.N. Ross Jr., in: E.E. Petersen, A.T. Bell (Eds.), Catalyst Deactivation, Marcel Dekker, New York, 1987, p. 165.
[10] C.H. Paik, G.S. Saloka, G.W. Graham, Electrochem. Solid-State Lett. 10 (2) (2007) B39.
[11] R.L. Borup, J.R. Davey, F.H. Garzon, D.L. Wood, M.A. Inbody, J. Power Sources 163 (2006) 76.
[12] R.L. Borup, J.R. Davey, F.H. Garzon, J. Power Sources 163 (2006) 76.
[13] M. Sogaard, M. Odgaard, E.M. Skou, Solid State Ionics 145 (2001) 31.
[14] D.A. Stevens, J.R. Dahn, J. Electrochem. Soc. 150 (2003) A770.
[15] H. Xu, R. Kunz, J.M. Fenton, Electrochem. Solid-State Lett. 10 (1) (2007) B1.
[16] H. Xu, Y. Song, H.R. Kunz, J.M. Fenton, J. Electrochem. Soc. 152 (2005) A1828.
[17] F.A. Uribe, T.A. Zawodzinski Jr., Electrochim. Acta 47 (2002) 3799.
[18] W. Bi, Q. Sun, Y. Deng, T.F. Fuller, Electrochim. Acta 54 (2009) 1826.
[19] C.H. Paik, T.D. Jarvi, W.E. O'Grady, Electrochem. Solid-State Lett. 7 (4) (2004) A82.
[20] A.Z. Weber, J. Newman, J. Electrochem. Soc. 150 (7) (2003) A1008.
[21] A. Ohma, S. Suga, S. Yamamoto, K. Shinohara, J. Electrochem. Soc. 154 (2007) B757.
[22] A. Ohma, S. Yamamoto, K. Shinohara, J. Power Sources 182 (2008) 39.